MAGNETIC NANOWIRE ARRAYS OBTAINED BY ELECTRO-DEPOSITION IN ORDERED ALUMINA TEMPLATES

K. Nielsch, F. Müller, G. Liu, R.B. Wehrspohn, U. Gösele,
S. F. Fischer and H. Kronmüller**
Max-Planck-Institut für Mikrostrukturphysik, Weinberg 2, 06120 Halle, Germany
* Max-Planck-Institut für Metallforschung, Heisenbergstr. 1, 70569 Stuttgart, Germany

Nickel and Cobalt nanowires were grown in highly ordered pores of anodic alumina membranes using pulsed electrodeposition. The hexagonally arranged pore matrices were fabricated by self-patterning in two successive anodization processes. Before the filling process, the insulating barrier layer at the bottom of the membrane was thinned homogeneously by current-limited anodization steps. During the deposition from a Watts bath two short millisecond deposition pulses were applied, followed by a comparatively long delay time to attain quite a high metal ion concentration at the deposition interface. This technique yielded completely metal-filled alumina membranes, which were analyzed by scanning electron microscopy and X-ray diffraction. The magnetic behavior of the metal-filled nano-pore arrays was characterized by SQUID-magnetometer measurements and the coupling between the nanowires was analyzed.

INTRODUCTION

Magnetic storage has played a key role in the development of the information technology. From 1956 to 1991, the areal density has progressed with an average rate of 23% per year. Since 1991, the growth rate of the storage density for commercially available hard disk has been 60%. Nowadays, hard disks with a areal density of 10.1 Gbit/in^2 are commercially available, and a number of companies have demonstrated densities ranging up to 35.5 Gbit/in^2 in their laboratories. Currently, it takes approximately two years from a laboratory demonstration to the market introduction. If the growth rate for areal densities continue the predicted superparamagnetic limit of about 40-70 Gbit/in^2 might be reached in products in a few years [1].

One approach to extend this limit is through patterned perpendicular media [2-6], where one information bit corresponds to one single-domain nanosized particle or so-called nanomagnet. Since each bit would be composed of a single large aspect particle (rather than ~1000 grains), the areal density of pattered media can, in principle, be much more than an order of magnitude greater than in conventional longitudinal media. For example, an areal density of about 300 Gbit/in^2 can be achieved by a hexagonal arranged array of nanomagnets with a lattice constant of about 50 nm.

The production of nanomagnet arrays based on hexagonal arranged porous alumina as a template material is cheaper than that based on traditional methods like nanoscaling using electron beam lithography [7]. Moreover, these arrays of magnetic nanowires can be easily fabricated over areas of several cm^2. We have shown recently that ordered porous alumina arrays can be obtained with a sharply defined pore diameter by a two-step electrochemical anodization process of aluminum. The interpore distance, the pore diameter and length can be varied over a large range [7-10]. For example, the interpore distance a can be adjusted between 50 –500 nm with the pore diameter d being controlled independently (with $d<a$).

For the deposition of the magnetic structures, the use of pulsed electrodeposition leads to uniform metal deposition in the pores of porous alumina templates with no direct metallic back contact as used in membrane structures. For this technique, the barrier layer of the porous alumina is thinned by current limited anodization. The advantage of this new method is that the porous alumina structure can stay on the aluminum substrate for the hole process and has not to be lifted off. The process allows the fabrication of thin films between 300 nm and 1 µm. This is of particular importance since thickness is a critical issue for compact magnetic devices. We have recently succeeded in a very homogeneous nickel filling of these highly ordered structures of porous alumina electro-depositing from a highly concentrated electrolyte (Watts bath) [7]. Our developed deposition process has been extended to other metals like iron and cobalt.

In the following, preparational aspects of the deposition of different magnetic materials in porous alumina are discussed. Moreover, a study of magnetic hysteresis of our metal-filled nano-pore arrays is presented here.

PREPARATION OF THE POROUS ALUMINA STRUCTURE

The hexagonally ordered porous alumina membranes have been prepared via a two-step anodization process, which is described in detail in Refs. 10 and 11. A first long-time anodization causes the formation of channel arrays with a high aspect ratio and regular pore arrangements via self-organization [8-14]. After complete dissolution of the oxide structure (Fig. 1 a), the surface of the aluminum substrate keeps the regular hexagonal texture of the self-organized pore tips, which act as self-assembled mask for a second anodization process. After a second anodization for 1 h, an ordered nanopore array (Fig. 1 b) is obtained with straight pores from top to bottom and a thickness of typically 1 µm. The parameters used here are 0.3 M oxalic acid, U_{ox}=40 V and T=2° C.

Thinning the barrier layer improves the quality and homogeneity of the deposition process in the pores significantly. The barrier layer has been thinned by chemical pore widening and by current-limited anodization steps: Firstly, the oxalic acid is heated up to 30 °C to decrease the thickness of the barrier layer by chemically widening the pores (Fig. 1 c). After 3 h, the barrier layer has decreased from 45 to 30 nm and the mean pore diameter has increased to approximately 50 nm. Afterwards, the electrolyte was cooled down to 2 °C to interrupt the widening process.

Secondly, the structure has been anodized twice for 15 minutes using constant current conditions of 290 and 135 mA/cm^2, respectively. During these anodization steps, the anodization potential decrease, the pores branch out at the formation front and the thickness of the barrier layer is reduced significantly. Finally, the anodizing potential has reached a value of 6 to 7 V, which corresponds to a barrier oxide thickness of less than 10 nm. A detail description of the pretreatment of the porous alumina structure for the filling process of the pores has been published in Ref. 7, recently.

FILLING OF THE PORES WITH MAGNETIC MATERIALS

Nickel, cobalt and iron were electro-deposited from aqueous electrolytes at the pore tip of our high aspect-ratio porous material (Fig. 1 e). All metals were deposited from an highly concentrated Watts-bath-type [15] electrolytes to achieve an high concentration of metal ions in each pore. The recipe for the nickel electrolyte is 300 g/l $NiSO_4 \bullet 6H_2O$, 45 g/l $NiCl_2 \bullet 6H_2O$, 45 g/l H_3BO_3, pH=4.5. The mixture for the cobalt deposition is similar and it has a pH value of 4.3. The recipe for the iron-containing electrolyte is 120 g/l $FeSO_4 \bullet 7H_2O$, 45 g/l H_3BO_3. The temperature of the electrolytes was kept at 35° C.

Typically, an alternating current (ac) signal is used for the deposition [5,6,16-18], when the porous alumina structure is kept on its aluminum substrate for the filling process. The metal is directly deposited upon the nearly isolating oxide barrier layer at the pore tips. Recently we have demonstrated that a pulsed electrodeposition concept (PED) is more suitable for a directly and homogeneous filling of the high-aspect-ratio porous alumina structures [7]. Here, a short technical description is given only.

The pore filling was based on modulated pulse signals in the ms-range. During the relatively long pulse of negative current [8 ms, I_{pulse}= -70 mA/cm^2] the metal is deposited on the pore ground. The measured voltage signal varies between -8 and -12 V. After the deposition pulse, a short pulse of positive polarization [2 ms, U_{pulse}=+4V] (Fig. 3 b) follows to interrupt the electric field at the deposition interface immediately. The relative long break time was inserted between the deposition pulses to refresh the ion concentration at the deposition interface, to let disappear the deposition by-products from the pore tips and to insure a stable pH value in each pore during deposition. Consequently, the delay time t_{off} improves the homogeneity of the deposition. The optimum delay-time for the deposition of nickel was t_{off} =990 ms, for cobalt and iron t_{off} =590 ms. The deposition was continued until the metal deposition reaches the top of the matrix structure.

CHARACTERIZATION OF THE FILLING MATERIAL

The filled alumina samples were examined by Scanning Electron Microscopy (SEM) to determine the degree of the pore filling and the extension of the metal nanowires. Thinning the filled porous alumina from the top reveals nanowires which end below the

matrix surface and are easy to be studied by SEM. Thinning the sample by a focused ion beam yielded a 100 nm deep and funnel-shaped excavation in the structure. Micrographs of the filled pores were taken outside the thinned area and at lowest point beneath the initial membrane surface.

Fig. 2 shows top view SEM micrographs of a highly ordered alumina pore structure filled with nickel. The measured pore diameter is between 45 and 55 nm and the pore distance is 100 nm. Fig. 2 (a) was taken of a region outside the thinned area. In some pores, the nickel nanowires were grown up to the pore opening. The lowest point of the excavation is shown (Fig. 2 b), where a layer of 100 nm has been removed from the 1 µm thick membrane.

Almost 100% of the pores are filled with nickel (Fig. 2 b). Away from this lowest level, where the structure was not thinned, few pores show a metal filling (Fig. 2 a). Nevertheless, comparing this micrograph (Fig. 2 a) with Fig. 2 (b), we see that still almost each pore of the alumina structure is filled with nickel. In the black colored pores in Fig. 2 (a) the nickel nanowires end beneath the pore opening. If we take into account that the thickness of the structure has decreased by only about 10% at the lowest etched level (Fig. 2 b), the lengths of the nickel nanowires are more than 90% (900 nm) of the membrane thickness, with slight fluctuations. This assumption is also supported by Fig. 2 (a), where the grey level of the filled pores shows slight fluctuations. The different grey levels are caused by nickel fillings, which end at (white) or a few nanometers below (grey) the matrix surface.

The crystallinity of these samples were further analyzed by X-ray diffraction (XRD). From the θ-2θ-scan we roughly estimated the average crystallite size using the Scherrer equation for round particles, yielding a particle diameters $D_p \approx 13$ nm for the Ni (111) peak and for the (200) peak. These values are in good agreement with data reported earlier for the PED of thin nickel films [19,20]. As expected, the nickel crystallites have a fcc lattice. In contrast, the cobalt filling has a hcp atomic lattice and their calculated average crystallite diameter is $D_P \approx 21$ nm for the (1000), (1010) and (1100) peak.

CHARACTERIZATION OF THE MAGNETIC BEHAVIOR

The metal-filled nano-pore arrays have been characterized by surface sensitive magneto-optical Kerr effect (MOKE) measurements to optimize the deposition process. The bulk magnetic properties have then been carefully investigated by superconducting quantum interference device (SQUID, Quantum Design-MPMS) magnetometer measurements. The field dependent magnetization hysteresis was measured for cobalt and nickel nanomagnet arrays at 5 K and 300 K and for the array of iron nanowires at 300 K.

Figure 3 shows a typical bulk magnetization hysteresis loop at 5 K, Fig. 3 (a) and 300 K, Fig. 3 (b) of hexagonally ordered Co nanowires with a pitch of 100 nm, a pore diameter of about 50 nm and a length of about 1 µm (add dot density). The external field has been applied parallel ($\parallel$) and perpendicular ($\perp$) to the long axes of the nanowires.

The hysteresis measured at 300 K with the magnetic field applied parallel to the cobalt wires, shows a low coercive field of 464 Oe. (Tab.1). The measurement with the external

field perpendicular to the Co columns shows a reduced coercive field of 265 Oe. The hysteresis loop indicates preferential magnetic orientation perpendicular to the wire axis. At 5 K the hysteresis exhibits for both measurement directions similar coercive fields of $H_C^{||}$ = 650 Oe and $H_C^{\perp}$= 505 Oe that are increased with respect to those of 300 K. A decrease of magnetic hardness with increasing temperature signals thermal demagnetization effects. The necessity of high external fields ($H_S \approx 4000 - 14000$ Oe) with respect to the coercive field, to reach the saturation value of the magnetization is an indication for a strong magnetic coupling of the nanowires.

Figure 4 shows the magnetization of hexagonally ordered Ni nanowires with a similar pitch of 100 nm, a pore diameter of about 50 nm and a length of 1 µm. The magnetic measurements were performed under the same conditions as mentioned above for the Co sample at 5 K (Fig. 4 (a)) and 300 K (Fig. 4 (b)). For the nickel filled sample a drastic difference of coercive field measured in applied field parallel and perpendicular to the column axis are observed at 300 K. While a parallel measurement exhibits a coercive field of about 600 Oe, a perpendicular measurement shows a value of only 112 Oe. At 5 K the coercive field for perpendicular measurement is given by 214 Oe in accordance with the behavior observed with the cobalt filled alumina template. For the parallel measurement the coercive field is decreased to 423 Oe at 5 K. The latter indicates a temperature dependent contribution to the competing magnetic interactions of the array of nickel nanowires, changing the magnetic anisotropy of the system. These values are at least a factor of 5-10 smaller than the values expected for a single domain wire magnetized parallel to the pore axis. It is therefore suggested that we deal with a multidomain structure of the wires and the coercive fields are determined by the pinning of domain wall type structures at grain boundaries.

In general the effective magnetic anisotropy of an array of thin magnetic wires results from the interplay of a series of effective fields. In the case of a single domain wire which in Ni is expected to be present for diameters smaller than 55 nm [21] we have to consider three contributions.

1. The macroscopic demagnetization field due to the average magnetic charges of the pores at the surface. For Ni and the geometry of the hexagonal pore structure this demagnetization field is of the order of −1.300 Oe for 50 nm pores and -640 Oe for 35 nm pores.
2. The form effect of the individual wire if magnetized parallel to the pore axis is of the order of $2 \pi M_S$ = 3.200 Oe.
3. A third contribution results from the magnetocrystalline anisotropy energy, given by $(-) 4 K_1 / 3 M_S \cong 120$ Oe for Ni.

A similar calculation could be performed for Fe and Co leading to much larger field values because of the larger spontaneous magnetizations and the larger anisotropy constants, e.g., in the case of co the form effects leads to a field of 8.800 Oe. Therefore in the case of Fe and Co we suggest to deal with multidomain structures of the wires. The situation is different for the Ni-pores with a diameter of 35 nm as shown in Fig. 5. Reducing the pore diameter from 50 to 35 nm while keeping the interpore distance

constant, the remanence indeed increases and the coercive field shifts towards 1000 Oe. A detailed report of the influence of the nanowire diameter on the magnetization of a nickel nanowire array will be published elsewhere [22]. For the Ni sample with a pore diameter of 35 nm we are sure to deal with single domain wires and the wires are preferentially magnetized parallel to the pore axes because the form effect of 3200 Oe overcomes easily the crystal field of only 120 Oe. The theoretical effective field responsible for the coercive field is given by the so-called nucleation field H_{eff} = (3.200-640) Oe = 2.560 Oe. The measured smaller coercive field of ~1.000 Oe may be explained by the existence of soft magnetic nuclei at the surface of the wires being due to imperfect crystalline structures as is well know from the hard magnetic materials. It is of interest that the hysteresis loop for H perpendicular to the pore axes results in a nearly reversible magnetization curve as predicted for the case of wires magnetized parallel to the pore axis. The saturation field of the order of 3.000 Oe agrees rather well with the field of 3.200 Oe of the form effect.

	coercive field [Oe]		saturation field [Oe]		squareness [%]		temperature
	B ll wire	B ⊥ wire	B ll wire	B ⊥ wire	B ll wire	B ⊥ wire	
Nickel	423	219	4.000	1.500	17,0	38,3	**5 K**
	600	112	2.500	2.500	28,3	9,0	**300 K**
Nickel*	990	130	2.300	6.000	78,0	6,5	**300 K**
Cobalt	650	505	14.000	6.000	8,7	39,7	**5 K**
	464	265	10.000	4.000	6,7	10,8	**300 K**
Iron	343	111	8.500	6.000	5,7	2,8	**300 K**

Tab. 1: Summary of the SQUID measurements on a Ni, Co and Fe filled alumina template with a 100 nm pitch, about 50 nm (*35 nm) pore diameter and 1 µm template thickness: coercive fields [H_c], saturation fields [H_s] and squareness [$M(H=0)/M(H_S)$].

The iron sample exhibits a magnetic behavior similar to the cobalt ones. The coercive fields for both measurement directions are very low with respect to the saturation fields. One additional demagnetization effect arises in the case of Fe from the fact that the critical single domain diameter is only 14.5 nm [21]. In contrast, Ni and Co have a much higher single domain diameter of about 55 and 65 nm, slightly larger than the typical pore diameter (≈ 50 nm). Thus, a multidomain state is anticipated in the iron samples whereas in the Co and Ni samples, one may assume a single domain state of magnetization. By reducing the Fe pore diameter below 15 nm, one might expect a higher coercive fields corresponding to a single domain particle, as indeed observed by Ref. 5 and 6.

As visible in Fig. 3 and 4 the magnetic hysteresis shows a broad field range of approach to saturation. Templates filled with Ni show the lowest saturation fields compared to those filled with Co or Fe. For application the squareness of the hysteresis loop has to be strongly increased, for which the ratio of the saturation field to coercive field gives a measure. From our measurements Ni or Ni-related soft magnetic alloys (Permalloy) appear the most promising candidates as filling materials of alumina templates with pore diameters below 35 nm, when the template structure has a pitch of 100 nm.

CONCLUSION

A highly efficient method of depositing nickel, cobalt and iron into ordered nano-channels of porous alumina has been presented. By thinning the barrier layer homogeneously, the porous structure could be kept on the aluminum substrate over the whole process. Our approach to fabricating a highly ordered metal nanowire array is inexpensive and very flexible with respect to the size and thickness of the pore structure. Nearly 100% of the pores were filled with nano-crystalline nickel, cobalt or iron implying only slight fluctuations in the growth rate of these nanowires. Bulk magnetic measurements were performed on the hexagonal ordered nickel, cobalt and iron nanomagnet system with a pitch of 100 nm and a wire diameter of about 50 nm at 5 K and 300 K. The array of Ni columns shows hysteresis loops with smaller coercive fields for perpendicular magnetization indicating the dominance of reversible rotation processes versus the anisotropy field of the form effect. In the case of Co this behaviour is less developed because a more or less isotropic domain structure exists. For the perpendicular storage media, nickel seems to be a suitable magnetic filling material for highly ordered porous alumina templates with a pitch of 100 nm. Reducing the pore diameter from 50 to 35 nm, while keeping the interpore distance constant, increases the squareness of the hysteresis loop and raises the coercive field to up 1000 Oe.

ACKNOWLEDGEMENT

The authors are grateful to Mrs. S. Hopfe for preparing the SEM samples and Dr. S. Senz and Mrs. S. Reichel for performing the x-ray measurements. The authors would like to thank Prof. J. Kirschner and Prof. H.-P.Oepen for fruitful discussions.

REFERENCES

1. D. Weller and A. Moser, *IEEE Trans. Magn.*, **35**, 4423 (1999).
2. C.A. Ross, H.I. Smith, T. Savas, M. Schattenberg, M. Farhoud, M. Hwang, M. Walsh, M.C. Abraham, and R.J. Ram, *J. Vac. Sci. Technol.,* **B 17**, 3159 (1999).
3. S.Y. Chou, M. Wei, P.R. Kraus, and P.B. Fisher, *J. Vac. Sci. Technol.*, **B 12**, 3695 (1994).
4. R, O'Barr, S.Y. Yamamoto, S. Schultz, W. Xu, and A. Scherer, *J. Appl. Phys.,* **81**, 4730 (1997).
5. D. Al Mawlawi, N. Coombs, and M. Moskovits, *J. Appl. Phys.*, **70**, 4421 (1991).
6. F. Li, R.M. Metzger, and W.D. Doyle, *IEEE Trans. Magn.*, **33**, 3715 (1997).
7. K. Nielsch, F. Müller, A.P. Li, and U. Gösele, *Adv. Mater.,* **12**, 582 (2000).
8. O. Jessensky, F. Müller, and U. Gösele, *J. Electrochem. Soc.*, 145, 3735 (1998).
9. A.P. Li, F. Müller, A. Birner, K. Nielsch, and U. Gösele, *J. Appl. Phys.*, **84**, 6023 (1998).
10. A.P. Li, F. Müller, A. Birner, K. Nielsch, and U. Gösele, *Adv. Mater.*, **11**, 483 (1999).
11. H. Masuda, and M. Satoh, *Jpn. J. Appl. Phys.,* **35**, L 126 (1996).
12. H. Masuda and K. Fukuda, *Science*, **268**, 1466 (1995).

13. H. Masuda, K. Yada, and A. Osaka, *Jpn. J. Appl. Phys.*, **37**, L 1340 (1998).
14. F. Li, L. Zhang, and R.M. Metzger, *Chem. Mater.,* **10**, 2473 (1998).
15. O. P. Watts, *Trans. Am. Electrochem. Soc.,* **29**, 395 (1916).
16. W. Sautter, G. Ibe and J. Meier, *Aluminium*, **50**, 143 (1974).
17. D. Routkevitch, A.A. Tager, J. Haruyama, D. Almawlawi, M. Moskovits, and J.M. Xu, *IEEE Trans. Electron Dev.,* **147**, 1646 (1996).
18. D. Routkevitch, J. Chan, J.M. Xu, and M. Moskovits, *The Electrochemical Society Proceedings Series*, **PV 97-7**, 350, Pennington, NJ (1997).
19. G. McMahon and U. Erb, *Microstruct. Sci.,* **17**, 447 (1989).
20. P.T. Tang, T. Watanabe, J.E.T. Andersen, and G. Bech-Nielsen, *J. Appl. Electrochem.,* **25,** 347 (1995).
21. G.J.Long and F.Grandjean, Supermagnets, Hardmagnetic Materials, p. 461-498, Kluwer Academic Publishers, NL (1991).
22. K. Nielsch, unpublished data.

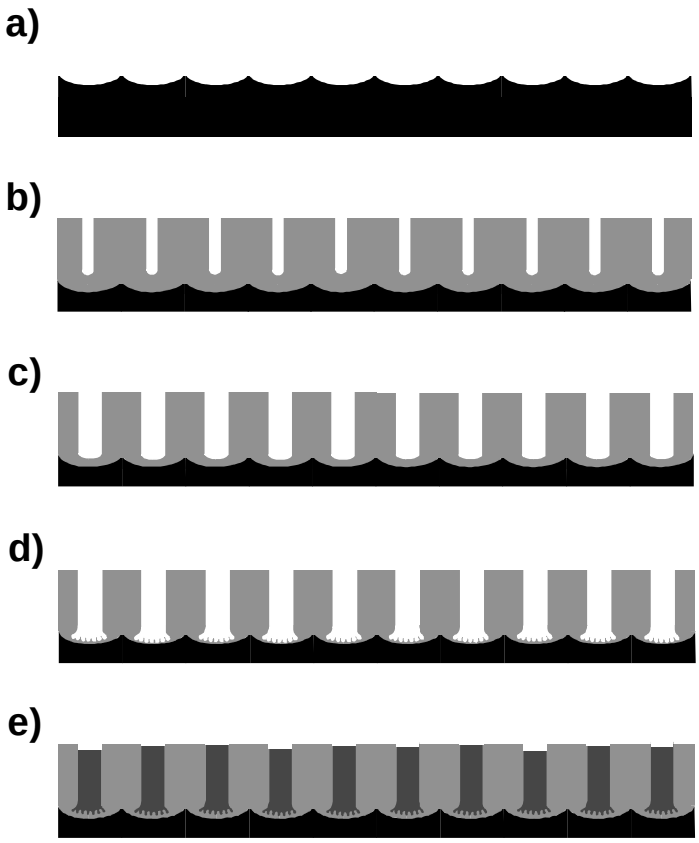

Fig. 1: Schematic diagram demonstrating the fabrication of a highly ordered porous alumina matrix and the preparational steps necessary for the subsequent filling of the structure. The Al-substrate was pre-structured by a long-time anodization and by removing the oxide (a). A second anodization step yielded a highly ordered alumina pore structure (b). The barrier layer was thinned and the pores were widened by isotropic chemical etching (c). To thin the barrier layer further, two current-limiting anodization steps followed, with dendrite pores forming at the barrier layer (d). Metal deposition in the pores (e).

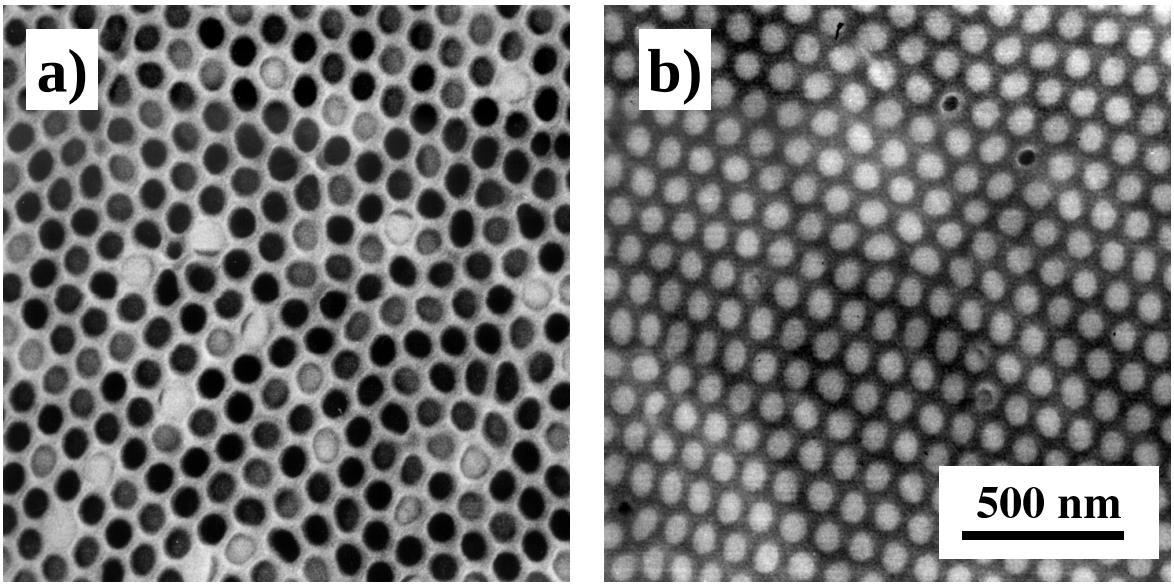

Fig. 2: Top-view SEM micrographs of a nickel-filled alumina membrane with a pitch of 100 nm, about 50 nm pore diameter and membrane thickness 1 µm; (a) un-thinned and (c) 100 nm underneath the initial surface.

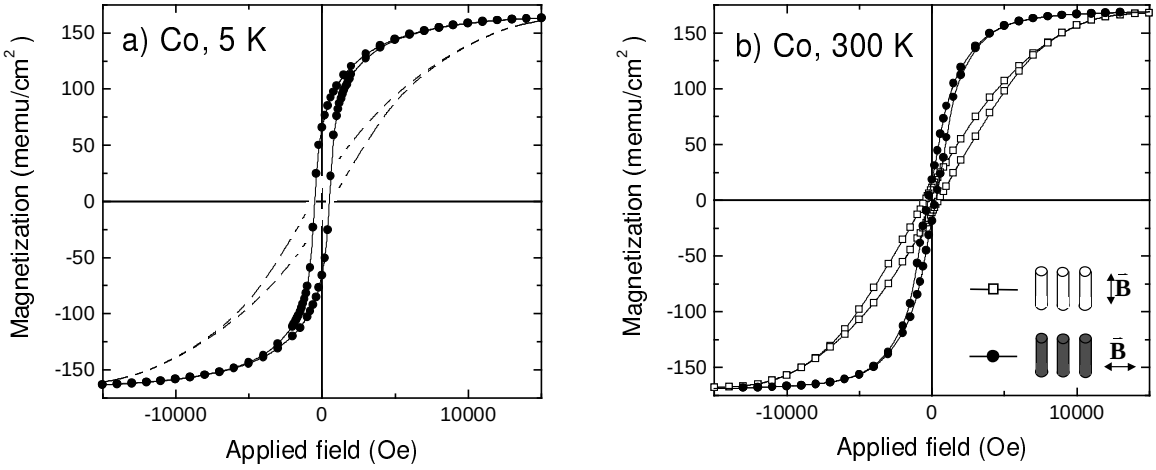

Fig. 3: SQUID hysteresis loop for a hexagonally ordered Co nanowire array with a pitch of 100 nm and a pore diameter ≈50 nm at 5 K (a) and at 300 K (b).

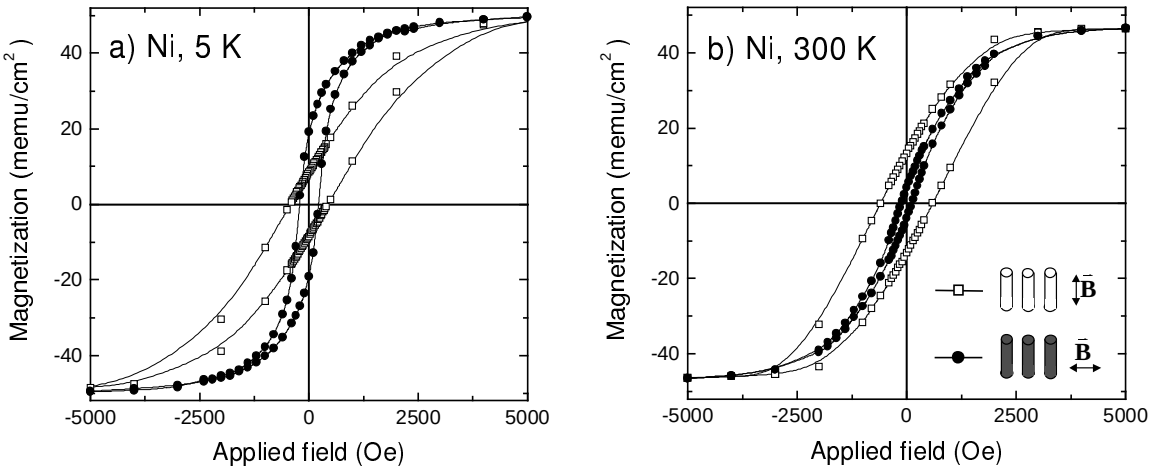

Fig. 4: SQUID hysteresis loop for a hexagonally ordered Ni nanowire array with a pitch of 100 nm and a pore diameter ≈50 nm at 5 K (a) and at 300 K (b).

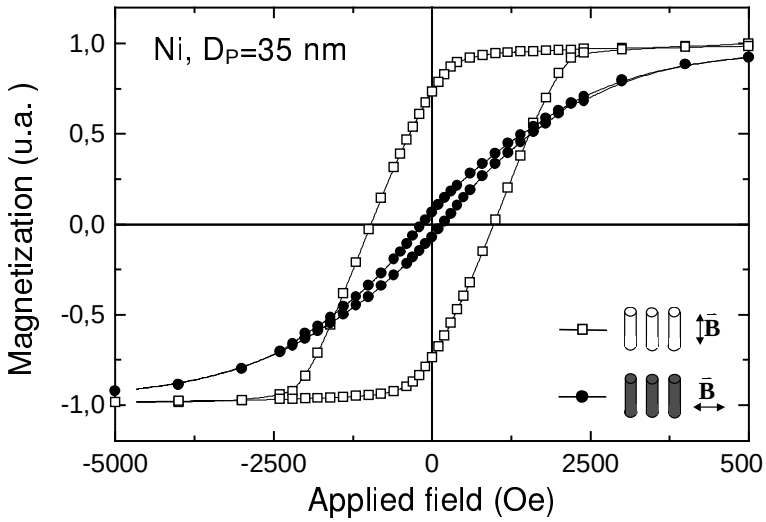

Fig. 5: SQUID hysteresis loops for an hexagonally ordered Ni nanowire array (100 nm pitch) with a pore diameter of 35 nm measured at 300 K.